ACS OMEGA

http://pubs.acs.org/journal/acsodf

Article

Amyloid and Tau Induce Cell Death Independently of TSPO Polymerization and Density Changes

Benjamin B. Tournier, Kelly Ceyzériat, Farha N. Bouteldja, and Philippe Millet*

Cite This: *ACS Omega* 2021, 6, 18719−18727

Read Online

ACCESS | Metrics & More | Article Recommendations

ABSTRACT: Apoptosis-dependent cell death of astrocytes has been described in Alzheimer's disease and is linked to the presence of two markers of the pathology: the β-amyloid peptide (Aβ) and the hyperphosphorylated Tau protein. Astrocytes also show reactive states characterized by the overexpression of the 18 kDa translocator protein (TSPO). However, TSPO is also known, in other areas of research, to participate in cell proliferation and death. Regulation of its function by autopolymerization has been described, but its involvement in apoptosis remains unknown. The aim was to determine the effects of Aβ, Tau, and TSPO antagonists on proliferation/cell death and TSPO polymerization in the C6 astrocytic cell line. The dose-effect on cell death in response to Aβ and Tau was observed but without alterations of TSPO density and polymerization. In contrast, nanomolar doses of antagonists stimulated cell proliferation, although micromolar doses induced cell death with a reduction in TSPO density and an increase in the ratio between the 36 and the 72 kDa TSPO polymers. Therefore, an alteration in the density and polymerization of TSPO appears to be related to cell death induced by TSPO antagonisms. In contrast, Aβ- and Tau-induced death seems to be independent of TSPO alterations. In conclusion, even if its role in cell death and proliferation is demonstrated, TSPO seems to, in the context of Alzheimer's disease, rather represent a marker of the activity of astrocytes than of cell death.

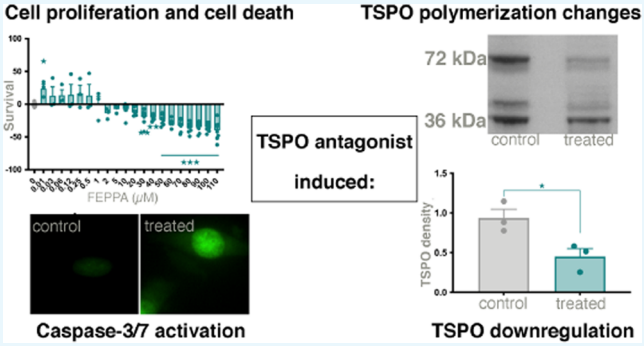

INTRODUCTION

Alzheimer's disease is characterized by the presence of pathological markers such as the accumulation of β amyloid (Aβ) in the extracellular environment and the intraneuronal formation of Tau neurofibrillary tangles (NFT). From a molecular point of view, many studies have focused on the search for pathological events affecting the functioning of neurons. For example, the presence of alterations in synapse activity, excitability of neurons, and an increase in neuronal death by apoptosis have been observed in response to Aβ as to Tau.[1−4] However, since amyloid and Tau can be released from neurons in the parenchyma,[5] their actions are not limited to neurons but also affect other surrounding cells. Among its many roles, microglia participate in the inflammatory reaction, phagocytose the amyloid, and release cytokines in response to stimulation.[6−8] Astrocytic cells are also involved in the uptake of amyloid[9] and Tau;[10,11] they show a modification of their activity linked to the density of amyloid and NFT[12] and participate in the induction of neuronal death in response to the presence of Aβ.[13] However, an increase in the apoptosis of astrocytes has also been described in relation with the presence of amyloid plaques.[14−17] The rat glial C6 cell cultures used in the present study can model this effect as amyloid exposure leads to cell death.[18]

An increase in the 18 kDa translocator protein (TSPO) was observed in glial cells from both preclinical rodent models and human AD.[19,20] In the 3xTgAD mouse model, TSPO does not appear to be a consequence of the accumulation of extracellular amyloid deposits, as it accumulates earlier.[21] However, it is still possible that the TSPO upregulation could be a consequence of the soluble amyloid already present at the time of TSPO accumulation.[22] In addition, we have shown that astrocytes overexpress TSPO before microglia, suggesting an earlier role of TSPO in astrocytes.[23] TSPO is supposed to reflect the activated states of glial cells but is also involved in cell death. Indeed, its inhibition by the presence of an antagonist induces death by apoptosis in different cell models. In the rat C6 cells, Rechichi et al. showed a dose-dependent (1−100 μM) induction of cell death using a 24 h treatment with one TSPO antagonist.[24] In another study, cell death by

Received: March 29, 2021
Accepted: June 29, 2021
Published: July 14, 2021

apoptosis was observed with an effect of the treatment duration (12−48 h) and the dose of antagonist (1−100 μM) used on the human astrocytoma cell line.[25] Cell growth inhibition is also reported at doses of 10−50 μM with the use of non-glial lines, such as various thyroid cancer cells.[26] Overall, these studies supposed a direct role of TSPO in cell death or survival, which could significantly impact the neurodegeneration processes observed in AD.

Importantly, TSPO exists in different forms of polymerization, from monomeric forms of 18 kDa to highly polymerized forms including 72 kDa tetramers,[27,28] which could influence its function. Indeed, it has been recently shown that the binding of cholesterol, one of the endogenous ligands of TSPO, causes a modification of the polymerization of TSPO toward monomeric forms.[29] The presence of inflammatory molecules in the culture medium of human colonic adenocarcinoma cell line HT-29 induces a shift in the ratio of trimer/dimer forms in favor of dimers,[30] suggesting that a pathological context could influence TSPO oligomerization and therefore its functions.

Thus, these observations suppose an early intervention of TSPO in Alzheimer's disease and, in particular, in the astrocytic cells. However, the implication of alterations in TSPO density and its state of polymerization in Aβ- and Tau-induced astrocyte death remains unknown. The aim of this study was to determine the effects of the presence of amyloid or Tau on cell survival and TSPO polymerization in the C6 astrocytic cell line. We also extended this approach to time- and dose-dependent effects of TSPO antagonists.

RESULTS

C6 Cells Display 36 and 72 kDa TSPO Polymers. The western blot visualization of TSPO forms on C6 cells indicated the existence of a dimeric form at 36 kDa, a multimeric form at 72 kDa, and the absence of the monomeric form at 18 kDa (Figure 1A). To validate the absence of the monomeric form of TSPO in C6, its presence was demonstrated in two other cell lines, GL26 glial and B16 melanoma cells (Figure 1B).

Aβ- and Tau-Induced Cell Deaths are Not Associated with TSPO Changes. The western blot characterization of the Aβ42 solution indicated that most of the Aβ42 were in an aggregated form (Figure 2A). Amyloid-induced cell death was dose-sensitive ($F_{11,50}$ = 21.73, p < 0.001; Figure 2A) with a nonsignificant effect of low doses (0.015−0.25 μM) and a significant effect for higher doses (0.5−20 μM, p < 0.001). For Tau, the western blot revealed that most of the Tau were in a monomeric form (Figure 2B). Tau also induced cell death with a dose-dependent effect ($F_{5,18}$ = 6.23, p < 0.01; Figure 2B). A post hoc test indicated a decrease in cell survival for all doses tested (0.015−0.25 μM) as compared to control cells (from p < 0.05 to p < 0.001). Representative examples of DAPI staining in amyloid-treated and control cells (Figure 2C) showed morphological characteristics of apoptotic cell death. In addition, activated caspase-3/7 staining is increased in Tau- and Aβ-treated cells, demonstrating cell death via apoptosis (Figure 2D). However, amyloid and Tau treatments did not modify the relative abundance of the 36 and the 72 kDa TSPO polymers ($F_{2,9}$ = 1.45, p > 0.05; Figure 2E,F). In addition, the total TSPO density was not affected by both amyloid and Tau ($F_{2,9}$ = 0.25, p > 0.05; Figure 2G).

High Concentrations of TSPO Antagonists Induced Time-Dependent Cell Death. A treatment of C6 cells during 1−4 days with 80 μM FEPPA, a TSPO antagonist, induced a cell death that is time-dependent (treatment effect: $F_{1,29}$ = 18.72, p < 0.001; duration of treatment effect: $F_{3,29}$ = 5.17, p < 0.01; treatment x duration of treatment interaction: $F_{3,29}$ = 5.17, p < 0.01; Figure 3A). A post hoc test indicated that FEPPA significantly reduced the % of survival at day 3 (p < 0.01) and day 4 (p < 0.001) as compared to control and between the 2nd and the 3rd day of treatment (p < 0.01).

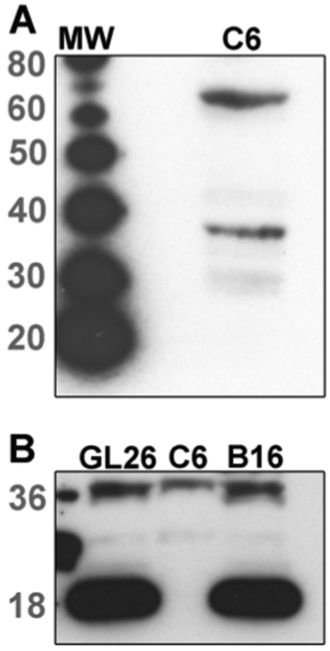

Figure 1. TSPO polymerization in C6, GL26, and B16 cells. (A) C6 cells showed two bands corresponding to 36 and 72 kDa TSPO polymers, whereas (B) GL26 and B16 cells displayed the monomeric 18 kDa TSPO form.

The experiment was duplicated using PBR28, another TSPO antagonist showing a high affinity for TSPO, but lower than FEPPA (4 vs 0.5 nM[31,32]), to validate that cell death was specifically induced by TSPO blockage. A 1−4-day treatment with 80 μM PBR28 also induced a time-dependent cell death (treatment effect: $F_{1,31}$ = 49.49, p < 0.001; duration of treatment effect: $F_{3,31}$ = 6.26, p < 0.01; treatment x duration of treatment interaction: $F_{3,31}$ = 6.26, p < 0.01; Figure 3A). A post hoc test indicated that PBR28 reduced the percentage of survival from the 2nd day (p < 0.05) to the 4th day of treatment (p < 0.001) as compared to control and the effect was amplified between the 2nd and the 3rd day (p < 0.01).

Representative examples of DAPI staining in the FEPPA-treated and control cells (Figure 3B) showed morphological characteristics of apoptotic cell death. In addition, activated caspase-3/7 staining is increased in FEPPA-treated cells (50 μM), demonstrating cell death via apoptosis (Figure 2C).

Low and High TSPO Antagonist Doses Stimulated and Inhibited Cell Survival, Respectively. To determine the dose-effect of TSPO antagonists on C6 survival, the cells were treated with a range of nanomolar and micromolar doses (0.01−110 μM) for 4 days. The one-way ANOVA indicated a significant impact of the FEPPA dose on cell survival ($F_{20,107}$ = 17.23, p < 0.0001; Figure 3D). A post hoc test showed that the low FEPPA dose stimulated cell survival (0.01 μM, p < 0.05), while moderate doses had no effect (0.03−20 μM), and the highest doses induced cell death (30−40 μM, p < 0.01; 50−110 μM, p < 0.001). These results were validated with the

https://doi.org/10.1021/acsomega.1c01678
ACS Omega 2021, 6, 18719−18727

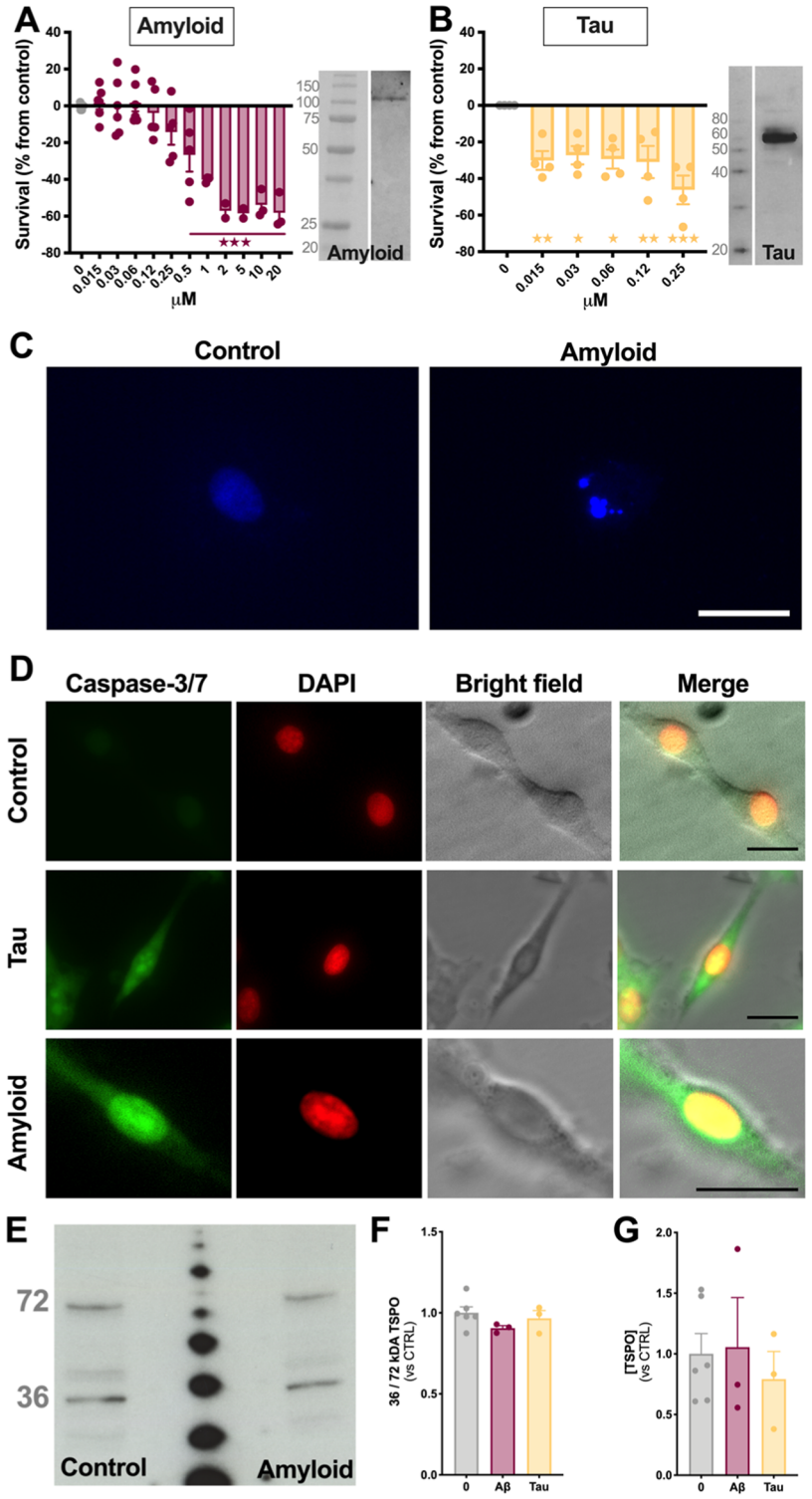

Figure 2. Amyloid- and Tau-induced cell death are not associated with TSPO changes. (A) C6 cells were treated with increasing concentrations of amyloid (0.015−20 μM) for 24 h. Cell survival was measured using the MTT assay and expressed as % from control. ***$p < 0.001$, as compared to untreated cells (two-way analysis of variance (ANOVA) with Dunnett's multiple comparisons post hoc test). Example of western blot examination of the amyloid solution demonstrating the aggregated form of Aβ42. (B) C6 cells were treated with increasing concentrations of Tau (0.015−0.25 μM) for 24 h. Cell survival was measured using the MTT assay and expressed as % from control. *$p < 0.05$; **$p < 0.01$; ***$p < 0.001$, as compared to untreated cells (two-way ANOVA with Dunnett's multiple comparisons post hoc test). Example of western blot examination of the Tau solution demonstrating the monomeric form of Tau. (C) Examples of DAPI staining in control and Aβ-treated cells demonstrate an apoptosis-like morphology. Scale bar: 20 μm. (D) Example of activated caspase-3/7 staining in control and Tau- and Aβ-treated cells to demonstrate the increase in caspase-3/7 showing an apoptosis-mediated cell death. Scale bars: 20 μm. (E) Examples of 36 and 72 kDa TSPO polymers in C6 cells treated with 1 μM Aβ for 24 h. The 36−72 kDa TSPO polymer ratio (F) and the TSPO density relative to total proteins (G) were quantified in control, 1 μM Aβ-treated cells, and 0.05 μM Tau-treated cells and expressed relative to the control group.

https://doi.org/10.1021/acsomega.1c01678
ACS Omega 2021, 6, 18719−18727

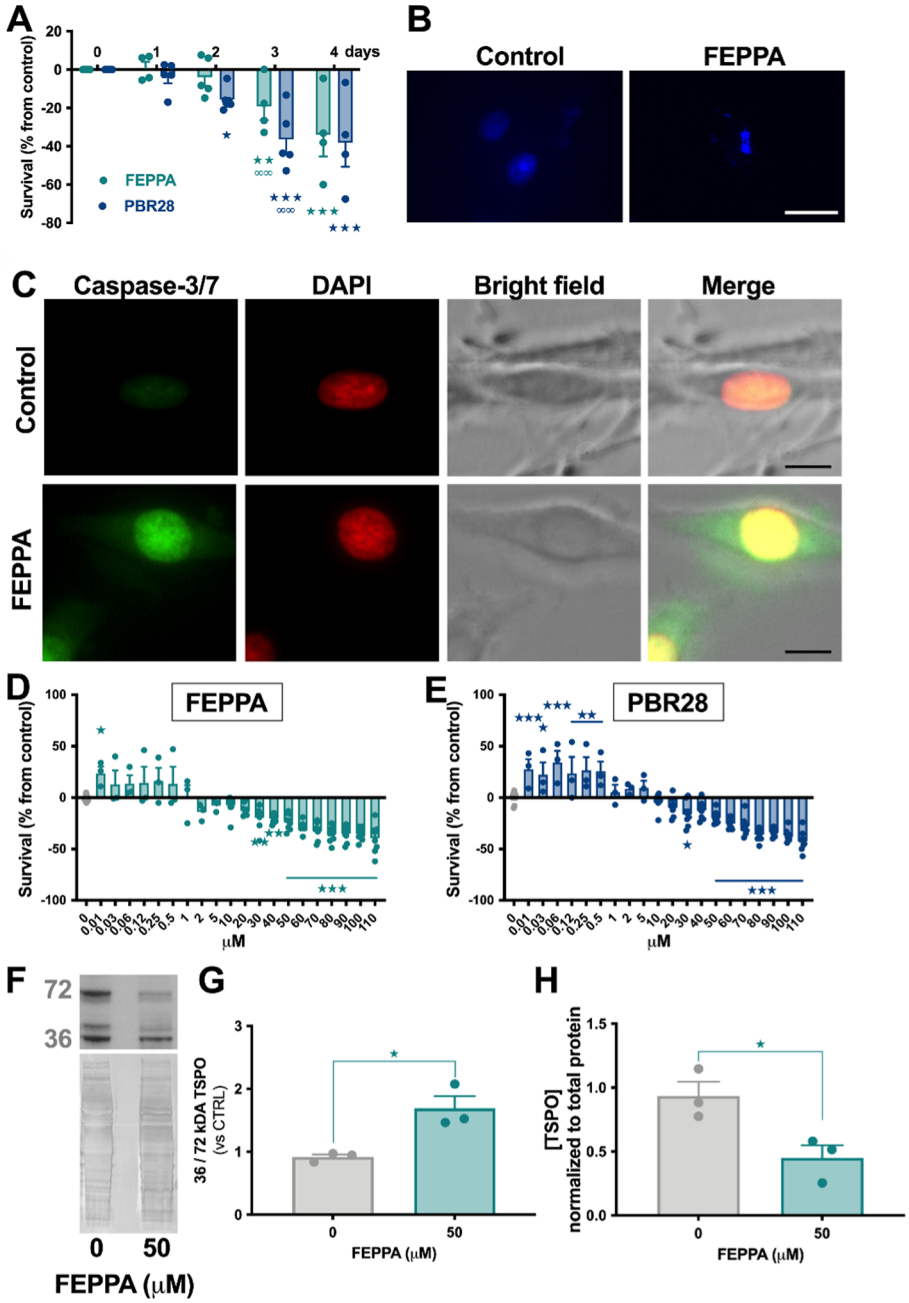

Figure 3. Time course of FEPPA- and PBR28-induced cell death. (A) C6 cells were treated with 80 μM FEPPA or PBR28 for 1−4 days. Cell survival was measured using the MTT assay and expressed as % from control. *$p < 0.05$; **$p < 0.01$; ***$p < 0.001$, as compared to untreated cells and $^{\#\#}p < 0.01$ as compared to the previous day (two-way ANOVA with LSD post hoc test). (B) Examples of DAPI staining (×400) at day 4 in control (left cell); FEPPA-treated cells demonstrate an apoptosis-like morphology (three right panels) Scale bar: 20 μm. (C) Example of activated caspase-3/7 staining in control and FEPPA-treated cells (50 μM) to demonstrate the increase in caspase-3/7 showing an apoptosis-mediated cell death. Scale bars: 20 μm. (D, E) C6 cells were treated with increasing concentrations of FEPPA or PBR28 (0.01−110 μM) for 4 days. Survival of FEPPA- (D) and PBR28-treated cells (E) was measured using the MTT assay and expressed as % from control. *$p < 0.05$; **$p < 0.01$; ***$p < 0.001$ (one-way ANOVA with the Dunnett's multiple comparisons post hoc test). (F) Examples of 36 and 72 kDa TSPO polymers (upper panel) and total proteins (DB71 staining, lower panel) in C6 cells treated with 0 or 50 μM FEPPA for 4 days. (G) Corresponding 36 to 72 kDa TSPO polymer ratio and (H) TSPO density relative to total proteins. *$p < 0.05$ (one-way ANOVA with the LSD post hoc test).

PBR28 treatment (Figure 3E). Indeed, one-way ANOVA also indicated the dose-effect on cell survival ($F_{20,107} = 27.58$, $p < 0.001$). The post hoc test showed that low PBR28 doses stimulated cell survival (0.01−0.5 μM, from $p < 0.05$ to $p < 0.001$), while moderate doses had no effect (1−20 and 40 μM) and the highest doses induced cell death (30 μM, $p < 0.05$; 50−110 μM, $p < 0.001$).

TSPO Antagonist-Induced Cell Death is Associated with TSPO Conformational and Density Changes. Since FEPPA and PBR28 have been shown to induce similar effects (i.e., stimulation of cell proliferation at nanomolar doses and cell death at micromolar doses), the effects on TSPO polymerization were only evaluated using FEPPA. To determine alterations on TSPO dimerization and density induced by a TSPO antagonism, the cells were treated with a

https://doi.org/10.1021/acsomega.1c01678
ACS Omega 2021, 6, 18719−18727

dose of FEPPA to induce cell death (Figure 3F−H). In response to FEPPA, the 36/72 kDa TSPO ratio was increased (*t*-test, $p < 0.05$) and the TSPO density was reduced (*t*-test, $p < 0.05$).

DISCUSSION

The study presented here aimed to determine whether TSPO used as a marker for neuroinflammation in many brain pathologies[19] also represents a marker for Aβ- and Tau-induced cell death in Alzheimer's disease. Our data show that in response to the presence of Aβ and Tau in the culture medium, the reduction of cell survival is not associated with either an alteration in the density or a change in the conformation of TSPO. However, stimulation of C6-type glial cells with micromolar doses of TSPO antagonists (FEPPA or PBR28) decreased cell survival in the presence of apoptosis. Conversely, a 4-day treatment with nanomolar doses of the same antagonists produced stimulation of cell proliferation. Importantly, during FEPPA-mediated apoptosis, there is a reduction of TSPO density and a shift toward the less complex forms of TSPO (from 72 to 36 kDa). These results suggest that a conformational change of TSPO may be associated with cell death. Overall, our data tend to support that in an Alzheimer's disease pathological context, TSPO does not seem to be implicated in the induction of astrocytic apoptosis by soluble forms of Aβ and Tau.

In cell cultures, TSPO is expressed by different glial lines such as glioma (C6, GL26) and glioblastoma cells.[24,33,34] The presence of the different TSPO forms appears to be cell line-dependent, and some possess while others are devoid of TSPO monomers.[26] Our data showed that C6 cells have the particularity of not possessing the monomeric form of TSPO. The specificity of cells to express a particular TSPO polymer has already been reported in other cell models.[26] The molecular mechanisms underlying these cell line differences and the impact on the control of cell physiology by TSPO remain unknown. However, this highlights that the role of TSPO in cell lines could depend on its polymerization. In line with this idea, the TSPO binding of cholesterol (one of the TSPO natural ligands) alters the level of TSPO polymerization.[29] It, therefore, appears important to interpret the molecular effects measured according to the type of cells studied. Thus, the data are presented here considering that the C6 glioma cell line is a representation of the astrocyte activity[35] and therefore simulates the astrocyte response to TSPO antagonisms, amyloid, and Tau.

In the brain of Alzheimer's disease subjects, an overexpression of TSPO in astrocytes and an astrocytic cell death by apoptosis is widely demonstrated in the absence of proliferation.[14−16,23,36] These effects are thought to be the result of the presence of amyloid and/or Tau in the cellular environment. Our data and others in the literature support this idea.[18] The effect of Tau on cell death seems to be insensitive to doses in the range of 0.015−0.12 μM. This absence of increasing cell death could be explained by an excessively tight Tau concentration range, thereby preventing a "point by point" dose-effect. However, both the literature (at higher Tau doses)[1] and the present ANOVA at low doses confirm the dose-dependent effect (clearly visible between 0 and the 0.015−0.12 μM range (−30%)) and a subsequent decrease at 0.25 μM (−45%).

In addition, the cell death induced by Tau and Aβ seems to be independent of any effect on TSPO density and polymerization. Although our analysis confirms that cell death is induced by Aβ and Tau, it remains speculative to conclude on the relative toxicity of Tau compared to Aβ. Indeed, in the brain, there are a variety of forms of Tau due to alternative splicing oligomerization and post-translational modifications, similar to a variety of forms of Aβ depending on the site of APP precursor cleavage and oligomerization.[37,38] The different forms may in themselves present different degrees of toxicity. For example, the soluble form of Tau induced greater neuronal death than the oligomerized forms of Tau.[39] As in the present report the Tau is monomeric, it may have a greater impact on cell death than the more complex forms would have had. Moreover, the soluble form of Aβ42 is more toxic to the neuronal culture model than the Aβ40 form.[40] Thus, only a comparative study would allow a full conclusion, but our data tend to show that the toxicity to C6 cells is greater in response to soluble Tau than to soluble amyloid. Since amyloid is in a multimeric form, its toxicity may have been altered compared to simpler forms. However, Aβ42 multimers have already been shown to have a biological impact, especially on DNA breaks,[41,42] suggesting a pathophysiological effect.[43] Some other factors can interact with TSPO, such as cholesterol. Interestingly, cholesterol and more generally the lipid metabolism are also affected in AD.[44] Lipid dyshomeostasis plays a role in amyloid production and inflammation and induces an unbalanced energy metabolism.[44,45] Thus, lipid dysfunction may play a role in the TSPO upregulation described in human and rodent models of AD[20] and in its mitochondria-based physiological processes, including cellular bioenergetics, mitochondrial respiration, cholesterol transport, and immunomodulation.[46]

Moreover, although FEPPA has approximately 10× greater affinity for TSPO than PBR28, induction of cell death occurs in both cases between 30 and 110 μM (except for the lack of significant effect at 40 μM for the PBR28). Conversely, the stimulating effect of cell viability is only present at a dose of 0.01 μM for FEPPA but present from 0.01 to 0.5 μM for PBR28. This difference could be explained by the stronger affinity of FEPPA, which would more quickly induce inhibition of the stimulation of proliferation. In addition, it was proposed that the ligand−TSPO interaction is governed not only by their direct interaction but also by the protein−complex composition and the cell-specific microenvironment inducing ligand-specific selectivity.[46] Nevertheless, despite those differences in affinity properties, the two ligands induce similar effects: stimulation of proliferation at low dose and inhibition at high dose. At low doses, TSPO antagonisms induce the stimulation of cell proliferation, which may reflect a tonic regulatory role of TSPO on cell proliferation. This hypothesis is supported by various experiments such as the presence of increased proliferation in a glioma model in response to TSPO knockout.[47] Stimulation of the growth of glioblastoma U118MG cells in response to the downregulation of TSPO also suggests an intrinsic inhibitory effect of TSPO.[48] However, in an interesting and opposite way, cells lacking TSPO exhibit increased proliferation by the addition of TSPO using a stable transfection of TSPO expressing plasmids.[49] TSPO-overexpressing C6 cells also show increased proliferation.[24] All of these data, therefore, seem in part contradictory, and further studies will be needed to decipher mechanisms of TSPO-induced cell proliferation or death.

At higher doses, TSPO antagonisms cause cell death that appears to be dose- and time-dependent. Cell death can also be

https://doi.org/10.1021/acsomega.1c01678
ACS Omega 2021, 6, 18719−18727

the result of side effects and nonspecific effects of drug administration. However, the involvement of TSPO in cell death is widely described and our data corroborate those obtained with other TSPO ligands, in the same dose range.[24,25] Thus, even if off-target effects cannot be completely excluded, a specific effect of ligands seems more likely. Thus, our data agree with those of the literature and extend them by the presence of an effect on the density and on the conformation of TSPO. The apoptosis induced by TSPO ligands[24,25,33] suggests that the decrease in density and the conformation shift toward less complex forms occur upstream of the onset of apoptosis and not as a consequence. This reduction in the complexity of the forms of TSPO was also observed in response to treatment for more than 24 h with the tumor necrosis factor (TNF).[30] A modification of the polymerization of TSPO may thus alter the apoptotic activity of TSPO, as has already been suggested for its other roles.[50] The molecular mechanisms of the control of cell death by TSPO are subject to discussion and may involve other molecular complexes including the mitochondrial permeability pore transition (mPTP).[51] How the interactions between tetramer, trimer, or monomer of TSPO and these protein complexes are regulated will have to be the subject of future studies to determine whether the simpler forms directly induce an increase in the proapoptotic activity of the mPTP pore for example.

As a limitation to this study, it appears important to point out that like all cell lines, C6 differs from the endogenous astrocytes that they represent,[35] and an analysis of astrocytes from animal models could prove to be important to confirm the data described herein. In addition, the toxicity of both amyloid and Tau differs according to their physical forms. Herein, no aggregation pretreatment was performed that suppose the use of monomeric peptides. Thus, the effects on TSPO polymerization and density must be interpreted with the limitation of the amyloid and Tau forms used. Therefore, future studies must be conducted to define whether Tau/amyloid oligomers and multimerization can affect TSPO.

In conclusion, although our data obtained with the antagonism of TSPO and the literature indicate that TSPO modifies the degree of apoptosis, we also demonstrated that TSPO polymerization may play a role in cell death, depending on the pathological context. Conversely, the presence of cell death in response to Tau and Aβ is independent of TSPO alteration (polymerization and density), suggesting that TSPO in Alzheimer's disease appears to better reflect its role in astrocyte reactivity than its role in apoptosis.

MATERIALS AND METHODS

Drugs. FEPPA and PBR28, two TSPO antagonists, were purchased from ABX (Radeberg, Germany), and amyloid was purchased from Enzolife Sciences (ALX-151-002-P001). Competition assay with the TSPO ligand [^{3}H]-PK11195 and unlabeled FEPPA, PBR28, and PK11195 made it possible to test the affinities (Ki) of these ligands for TSPO. The Ki was 0.5 nM for FEPPA and about 10 times less for PBR28 (4 nM).[31,32] However, both FEPPA and PBR28 have a high affinity as compared to PK11195 (26 nM).[32]

Tau Production. The complete coding sequence of human Tau was cloned with mRNAs extracted from the human cortex brain sample and primers allowing the addition of six histidine residues at the start of the sequence (NCBI Reference Sequence: BC114948; primers: for CACCATG-(CAT)$_5$CACGCTGAGCCCCGCCAGGAGTT; rev TCA-CAAACCCTGCTTGGCCAGGGA). After cloning into Gateway system entry vectors (pENTR), the full-length human Tau coding DNA sequence was inserted into pAd/CMV/V5-DEST adenoviral vectors, under the control of a cytomegalovirus promoter, thanks to LR recombination, according to the manufacturer's protocol (ViraPower Adenovirus Expression System, Invitrogen). Recombinant adenoviruses were sequenced to validate the presence of the complete human Tau sequence. Transfected HEK 293A cells permitted to amplify the AAV stores. Viral particles were then purified using the Vivapure AdenoPACK Sartorius kit (AVPQ501, Sartorius), quantified with the QuickTiter adenovirus titer kit (VPK-109, Cell Biolabs), and stored at −80 °C until use. A 3-day contamination period with 100 μL of AAV was used to extract the Tau-HIS from cells. Following purification (Ni-NTA purification system, Novex) and concentration (Amicon 10 K, Merck Millipore) steps, the Tau-HIS peptides were quantified by spectrophotometry, validated by western blot with the HT7 antibody (Thermo Scientific, MN1000), and stored at −80 °C until use.

C6 Cell Culture and Treatments. Rat C6 cells (Sigma-Aldrich) were cultured in a complete medium, including RPMI 1640 (Thermofisher, 31870025) with 10% FCS (Thermofisher, 16000044), 3% penicillin/streptomycin, 2 mM L-glutamine (Thermofisher, 25030024), 1% sodium pyruvate (Thermofisher, 11360039), and 2% HEPES (Thermofisher, 15630056) at 37 °C with 5% CO_2. The cells were subcultured after reaching 70−80% confluence and seeded into 6- or 96-well tissue culture plates at a density of 60 000 and 3000 cells/well, respectively. Six hours after distribution into wells, the cells were treated with FEPPA or PBR28. The cell medium and TSPO antagonists were renewed every day. For treatment with amyloid or Tau, the cells were cultured for 3 days and then exposed for 24 h to increasing doses of amyloid or Tau. β-amyloid (A$\beta_{1\text{-}42}$) was diluted in the complete medium at 1 mM and stored at −20 °C until use. Frozen stocks of amyloid and Tau (in 8 mM imidazole) were diluted daily in the complete medium and immediately used to treat cells. Control cells received the dilution solution of the compound to be tested as follows: complete medium alone (amyloid) or supplemented with 0.3% ethyl acetate (FEPPA/PBR28) or 8 mM imidazole (Tau).

MTT Assay. The cell viability was evaluated by the methyl thiazolyl tetrazolium (MTT) assay. C6 cells were incubated with MTT (0.8 mg/mL, Sigma-Aldrich, M2128) for 4 h. Cell culture media were removed and 150 μL of dimethyl sulfoxide (DMSO) (Sigma-Aldrich, D2650) was added to the wells to dissolve the purple complex. The absorbance was measured using an ELISA lector at 570 nm. Effects of treatments are expressed as percentage of controls.

Activated Caspase 3/7 Detection. C6 cells were plated at a density of 2 × 10^5 cells/well on Nunc Lab-Tek chamber slides. The cells were treated with A$\beta_{1\text{-}42}$ (5 μM), Tau (0.03 μM), and FEPPA (50 μM) for 24 h, and the untreated cells were used as controls. The cells were fixed in 4% paraformaldehyde (10 min at 4 °C) and a DAPI nuclei counterstaining was performed. The cells were incubated for 30 min in CellEvent Caspase-3/7 Green Detection Reagent (5 μM in 1× phosphate-buffered saline (PBS), Thermofisher). Images were taken using a microscope (ECLIPSE Ti2-E Nikon inverted microscope).

https://doi.org/10.1021/acsomega.1c01678
ACS Omega 2021, 6, 18719−18727

Western Blot. At the end of the treatment, C6 cells were lysed in 50 μL of extraction buffer (RIPA with protease and phosphatase inhibitors) and stirred for 45 min at 4 °C. The cells were then centrifuged (9500*g*, 10 min) and the supernatant was stored at −80 °C. The protein concentration was determined according to a BCA manufacturer protocol (Pierce, 23227). Thirty micrograms of extracted proteins treated with LDS (final concentration 1×, NP0007, Thermofisher) was used for the migration and transfer of the proteins in the presence of NNP0001 and NNP0006 buffers (Thermofisher), respectively. The poly(vinylidene difluoride) (PVDF) membrane was saturated with 5% skimmed milk for 1 h and then the TSPO antibody (1/500, Thermofisher, PA5-75544) was added overnight at 4 °C with stirring. An ECL detection was performed after adding a secondary antibody (1/1000, HRP-rabbit, Dako) for 1 h at RT. Washing steps (2 × 10 min in 0.2% Tween, 1× PBS) were carried out between each step. After the development of the membrane, it was treated with DB71 to quantify the total deposited proteins. The ImageJ Gel Analysis plugin was used to quantify the intensity of staining by measuring the area under the curve of the different TSPO forms. The same method was used to quantify the total level of proteins (DB71 staining). Then, ratios of intensities between the 32 kDa polymer and the 72 kDa polymer and between the total TSPO polymers and total proteins were calculated to evaluate the polymerization status and the relative density of TSPO, respectively.

Five micrograms of Aβ42 protein and 10 μg of Tau were also used for western blot evaluation of the forms of the peptides. Migration, transfer, and membrane pretreatment were performed as described above. 4G8 (1/500, Biolegend, 800710) and HT7 (1/500, Thermofisher, MN1000) antibodies were incubated for 48 h at 4 °C, washed, and incubated with the appropriate secondary antibodies before ECL detection. The molecular weight used on the Aβ42 blot was detected by fluorescence (Precision Plus Protein All Blue Prestained Protein Standards), and the ladder on the Tau membrane was revealed by ECL (SuperSignal Molecular Weight Protein Ladder).

Statistics. One and two-way analysis of variance (ANOVA) with the LSD or Dunnett's multiple comparisons post hoc test were used to identify significant effects of treatment. Data are presented as individual values plus mean ± standard error of the mean (SEM) of 3−6 independent experiments for cell survival (each experiment consists of triplicate, per dose) and mean ± SEM of three independent experiments for western blot.

AUTHOR INFORMATION

Corresponding Author

Philippe Millet − *Department of Psychiatry, University Hospitals of Geneva, 1205 Genève, Switzerland; Department of Psychiatry, University of Geneva, 1211 Genève, Switzerland*; Phone: +41 79 553 6376; Email: philippe.millet@hcuge.ch

Authors

Benjamin B. Tournier − *Department of Psychiatry, University Hospitals of Geneva, 1205 Genève, Switzerland; Department of Psychiatry, University of Geneva, 1211 Genève, Switzerland*; orcid.org/0000-0002-8027-7530

Kelly Ceyzériat − *Department of Psychiatry, University Hospitals of Geneva, 1205 Genève, Switzerland; Department of Psychiatry, University of Geneva, 1211 Genève, Switzerland; Division of Nuclear Medicine and Molecular Imaging, Diagnostic Department and Division of Radiation Oncology, Department of Oncology, University Hospitals of Geneva, 1205 Genève, Switzerland*

Farha N. Bouteldja − *Department of Psychiatry, University Hospitals of Geneva, 1205 Genève, Switzerland; Department of Psychiatry, University of Geneva, 1211 Genève, Switzerland*

Complete contact information is available at: https://pubs.acs.org/10.1021/acsomega.1c01678

Funding

No funding.

Notes

The authors declare no competing financial interest.

ACKNOWLEDGMENTS

The authors thank Maria Surini, Carline Meylan, and Anaïs Frisa for their technical assistance. Authors B.B.T. and K.C. are supported by the Velux Foundation (project no. 1123). This work was supported by the Swiss National Science Foundation (no. 320030-184713).

REFERENCES

(1) Gómez-Ramos, A.; Diaz-Hernandez, M.; Cuadros, R.; Hernandez, F.; Avila, J. Extracellular tau is toxic to neuronal cells. *FEBS Lett.* **2006**, *580*, 4842−4850.

(2) Wang, Y.; Mattson, M. P. L-type Ca2+ currents at CA1 synapses, but not CA3 or dentate granule neuron synapses, are increased in 3xTgAD mice in an age-dependent manner. *Neurobiol. Aging* **2014**, *35*, 88−95.

(3) Cordella, A.; Krashia, P.; Nobili, A.; Pignataro, A.; La Barbera, L.; Viscomi, M. T.; Valzania, A.; Keller, F.; Ammassari-Teule, M.; Mercuri, N. B.; Berretta, N.; D'Amelio, M. Dopamine loss alters the hippocampus-nucleus accumbens synaptic transmission in the Tg2576 mouse model of Alzheimer's disease. *Neurobiol. Dis.* **2018**, *116*, 142−154.

(4) Reiss, A. B.; Arain, H. A.; Stecker, M. M.; Siegart, N. M.; Kasselman, L. J. Amyloid toxicity in Alzheimer's disease. *Rev. Neurosci.* **2018**, *29*, 613−627.

(5) Yamada, K. Extracellular Tau and Its Potentia l Role in the Propagation of Tau Pathology. *Front. Neurosci.* **2017**, *11*, No. 667.

(6) Ceyzériat, K.; Ben Haim, L.; Denizot, A.; Pommier, D.; Matos, M.; Guillemaud, O.; Palomares, M. A.; Abjean, L.; Petit, F.; Gipchtein, P.; Gaillard, M. C.; Guillermier, M.; Bernier, S.; Gaudin, M.; Auregan, G.; Josephine, C.; Dechamps, N.; Veran, J.; Langlais, V.; Cambon, K.; Bemelmans, A. P.; Baijer, J.; Bonvento, G.; Dhenain, M.; Deleuze, J. F.; Oliet, S. H. R.; Brouillet, E.; Hantraye, P.; Carrillo-de Sauvage, M. A.; Olaso, R.; Panatier, A.; Escartin, C. Modulation of astrocyte reactivity improves functional deficits in mouse models of Alzheimer's disease. *Acta Neuropathol. Commun.* **2018**, *6*, No. 104.

(7) Baik, S. H.; Kang, S.; Son, S. M.; Mook-Jung, I. Microglia contributes to plaque growth by cell death due to uptake of amyloid beta in the brain of Alzheimer's disease mouse model. *Glia* **2016**, *64*, 2274−2290.

(8) Hickman, S.; Izzy, S.; Sen, P.; Morsett, L.; El Khoury, J. Microglia in neurodegeneration. *Nat. Neurosci.* **2018**, *21*, 1359−1369.

(9) Garwood, C. J.; Ratcliffe, L. E.; Simpson, J. E.; Heath, P. R.; Ince, P. G.; Wharton, S. B. Review: Astrocytes in Alzheimer's disease and other age-associated dementias: a supporting player with a central role. *Neuropathol. Appl. Neurobiol.* **2017**, *43*, 281−298.

(10) Perea, J. R.; Lopez, E.; Diez-Ballesteros, J. C.; Avila, J.; Hernandez, F.; Bolos, M. Extracellular Monomeric Tau Is Internalized by Astrocytes. *Front. Neurosci.* **2019**, *13*, No. 442.

(11) Söllvander, S.; Nikitidou, E.; Brolin, R.; Soderberg, L.; Sehlin, D.; Lannfelt, L.; Erlandsson, A. Accumulation of amyloid-beta by astrocytes result in enlarged endosomes and microvesicle-induced apoptosis of neurons. *Mol. Neurodegener.* **2016**, *11*, No. 38.
(12) Acosta, C.; Anderson, H. D.; Anderson, C. M. Astrocyte dysfunction in Alzheimer disease. *J. Neurosci. Res.* **2017**, *95*, 2430−2447.
(13) Garwood, C. J.; Pooler, A. M.; Atherton, J.; Hanger, D. P.; Noble, W. Astrocytes are important mediators of Abeta-induced neurotoxicity and tau phosphorylation in primary culture. *Cell Death Dis.* **2011**, *2*, No. e167.
(14) Yao, Y.; Huang, J. Z.; Chen, Y.; Hu, H. J.; Tang, X.; Li, X. Effects and mechanism of amyloid beta1-42 on mitochondria in astrocytes. *Mol. Med. Rep.* **2018**, *17*, 6997−7004.
(15) Saha, P.; Biswas, S. C. Amyloid-beta induced astrocytosis and astrocyte death: Implication of FoxO3a-Bim-caspase3 death signaling. *Mol. Cell. Neurosci.* **2015**, *68*, 203−211.
(16) Perez-Nievas, B. G.; Serrano-Pozo, A. Deciphering the Astrocyte Reaction in Alzheimer's Disease. *Front. Aging Neurosci.* **2018**, *10*, No. 114.
(17) Kobayashi, K.; Hayashi, M.; Nakano, H.; Shimazaki, M.; Sugimori, K.; Koshino, Y. Correlation between astrocyte apoptosis and Alzheimer changes in gray matter lesions in Alzheimer's disease. *J. Alzheimers Dis.* **2005**, *6*, 623−632. discussion 673-81
(18) Bashir, M.; Parray, A. A.; Baba, R. A.; Bhat, H. F.; Bhat, S. S.; Mushtaq, U.; Andrabi, K. I.; Khanday, F. A. beta-Amyloid-evoked apoptotic cell death is mediated through MKK6-p66shc pathway. *NeuroMol. Med.* **2014**, *16*, 137−149.
(19) Nutma, E.; Ceyzeriat, K.; Amor, S.; Tsartsalis, S.; Millet, P.; Owen, D. R.; Papadopoulos, V.; Tournier, B. B. Cellular sources of TSPO expression in healthy and diseased brain *Eur. J. Nucl. Med. Mol. Imaging* 2020, DOI: 10.1007/s00259-020-05166-2.
(20) Tournier, B. B.; Tsartsalis, S.; Ceyzeriat, K.; Garibotto, V.; Millet, P. In Vivo TSPO Signal and Neuroinflammation in Alzheimer's Disease. *Cells* **2020**, *9*, No. 1941.
(21) Tournier, B. B.; Tsartsalis, S.; Rigaud, D.; Fossey, C.; Cailly, T.; Fabis, F.; Pham, T.; Gregoire, M. C.; Kovari, E.; Moulin-Sallanon, M.; Savioz, A.; Millet, P. TSPO and amyloid deposits in sub-regions of the hippocampus in the 3xTgAD mouse model of Alzheimer's disease. *Neurobiol. Dis.* **2019**, *121*, 95−105.
(22) Oddo, S.; Caccamo, A.; Shepherd, J. D.; Murphy, M. P.; Golde, T. E.; Kayed, R.; Metherate, R.; Mattson, M. P.; Akbari, Y.; LaFerla, F. M. Triple-transgenic model of Alzheimer's disease with plaques and tangles: intracellular Abeta and synaptic dysfunction. *Neuron* **2003**, *39*, 409−421.
(23) Tournier, B. B.; Tsartsalis, S.; Ceyzeriat, K.; Fraser, B. H.; Gregoire, M. C.; Kovari, E.; Millet, P. Astrocytic TSPO Upregulation Appears Before Microglial TSPO in Alzheimer's Disease. *J. Alzheimer's Dis.* **2020**, *77*, 1043−1056.
(24) Rechichi, M.; Salvetti, A.; Chelli, B.; Costa, B.; Da Pozzo, E.; Spinetti, F.; Lena, A.; Evangelista, M.; Rainaldi, G.; Martini, C.; Gremigni, V.; Rossi, L. TSPO over-expression increases motility, transmigration and proliferation properties of C6 rat glioma cells. *Biochim. Biophys. Acta, Mol. Basis Dis.* **2008**, *1782*, 118−125.
(25) Chelli, B.; Salvetti, A.; Da Pozzo, E.; Rechichi, M.; Spinetti, F.; Rossi, L.; Costa, B.; Lena, A.; Rainaldi, G.; Scatena, F.; Vanacore, R.; Gremigni, V.; Martini, C. PK 11195 differentially affects cell survival in human wild-type and 18 kDa translocator protein-silenced ADF astrocytoma cells. *J. Cell. Biochem.* **2008**, *105*, 712−723.
(26) Klubo-Gwiezdzinska, J.; Jensen, K.; Bauer, A.; Patel, A.; Costello, J., Jr; Burman, K. D.; Wartofsky, L.; Hardwick, M. J.; Vasko, V. V. The expression of translocator protein in human thyroid cancer and its role in the response of thyroid cancer cells to oxidative stress. *J. Endocrinol.* **2012**, *214*, 207−216.
(27) Papadopoulos, V.; Baraldi, M.; Guilarte, T. R.; Knudsen, T. B.; Lacapere, J. J.; Lindemann, P.; Norenberg, M. D.; Nutt, D.; Weizman, A.; Zhang, M. R.; Gavish, M. Translocator protein (18 kDa): new nomenclature for the peripheral-type benzodiazepine receptor based on its structure and molecular function. *Trends Pharmacol. Sci.* **2006**, *27*, 402−409.
(28) Veenman, L.; Papadopoulos, V.; Gavish, M. Channel-like functions of the 18-kDa translocator protein (TSPO): regulation of apoptosis and steroidogenesis as part of the host-defense response. *Curr. Pharm. Des.* **2007**, *13*, 2385−2405.
(29) Jaipuria, G.; Leonov, A.; Giller, K.; Vasa, S. K.; Jaremko, L.; Jaremko, M.; Linser, R.; Becker, S.; Zweckstetter, M. Cholesterol-mediated allosteric regulation of the mitochondrial translocator protein structure. *Nat. Commun.* **2017**, *8*, No. 14893.
(30) Issop, L.; Ostuni, M. A.; Lee, S.; Laforge, M.; Peranzi, G.; Rustin, P.; Benoist, J. F.; Estaquier, J.; Papadopoulos, V.; Lacapere, J. J. Translocator Protein-Mediated Stabilization of Mitochondrial Architecture during Inflammation Stress in Colonic Cells. *PLoS One* **2016**, *11*, No. e0152919.
(31) Berroterán-Infante, N.; Balber, T.; Furlinger, P.; Bergmann, M.; Lanzenberger, R.; Hacker, M.; Mitterhauser, M.; Wadsak, W. [(18)F]FEPPA: Improved Automated Radiosynthesis, Binding Affinity, and Preliminary in Vitro Evaluation in Colorectal Cancer. *ACS Med. Chem. Lett.* **2018**, *9*, 177−181.
(32) Owen, D. R.; Howell, O. W.; Tang, S. P.; Wells, L. A.; Bennacef, I.; Bergstrom, M.; Gunn, R. N.; Rabiner, E. A.; Wilkins, M. R.; Reynolds, R.; Matthews, P. M.; Parker, C. A. Two binding sites for [3H]PBR28 in human brain: implications for TSPO PET imaging of neuroinflammation. *J. Cereb. Blood Flow Metab.* **2010**, *30*, 1608−1618.
(33) Zeno, S.; Zaaroor, M.; Leschiner, S.; Veenman, L.; Gavish, M. CoCl(2) induces apoptosis via the 18 kDa translocator protein in U118MG human glioblastoma cells. *Biochemistry* **2009**, *48*, 4652−4661.
(34) Tsartsalis, S.; Dumas, N.; Tournier, B. B.; Pham, T.; Moulin-Sallanon, M.; Gregoire, M. C.; Charnay, Y.; Millet, P. SPECT imaging of glioma with radioiodinated CLINDE: evidence from a mouse GL26 glioma model. *EJNMMI Res.* **2015**, *5*, No. 9.
(35) Galland, F.; Seady, M.; Taday, J.; Smaili, S. S.; Goncalves, C. A.; Leite, M. C. Astrocyte culture models: Molecular and function characterization of primary culture, immortalized astrocytes and C6 glioma cells. *Neurochem. Int.* **2019**, *131*, No. 104538.
(36) Tournier, B. B.; Tsartsalis, S.; Ceyzeriat, K.; Medina, Z.; Fraser, B. H.; Gregoire, M. C.; Kovari, E.; Millet, P. Fluorescence-activated cell sorting to reveal the cell origin of radioligand binding. *J. Cereb. Blood Flow Metab.* **2020**, *40*, 1242−1255.
(37) Ceyzériat, K.; Zilli, T.; Millet, P.; Frisoni, G. B.; Garibotto, V.; Tournier, B. B. Learning from the Past: a Review of Clinical Trials Targeting Amyloid, Tau and Neuroinflammation in Alzheimer's Disease. *Curr. Alzheimer Res.* **2020**, *17*, 112−125.
(38) Sebastián-Serrano, Á.; de Diego-Garcia, L.; Diaz-Hernandez, M. The Neurotoxic Role of Extracellular Tau Protein. *Int. J. Mol. Sci.* **2018**, *19*, No. 998.
(39) d'Orange, M.; Auregan, G.; Cheramy, D.; Gaudin-Guerif, M.; Lieger, S.; Guillermier, M.; Stimmer, L.; Josephine, C.; Herard, A. S.; Gaillard, M. C.; Petit, F.; Kiessling, M. C.; Schmitz, C.; Colin, M.; Buee, L.; Panayi, F.; Diguet, E.; Brouillet, E.; Hantraye, P.; Bemelmans, A. P.; Cambon, K. Potentiating tangle formation reduces acute toxicity of soluble tau species in the rat. *Brain* **2018**, *141*, 535−549.
(40) El-Agnaf, O. M.; Mahil, D. S.; Patel, B. P.; Austen, B. M. Oligomerization and toxicity of beta-amyloid-42 implicated in Alzheimer's disease. *Biochem. Biophys. Res. Commun.* **2000**, *273*, 1003−1007.
(41) Gruz-Gibelli, E.; Chessel, N.; Allioux, C.; Marin, P.; Piotton, F.; Leuba, G.; Herrmann, F. R.; Savioz, A. The Vitamin A Derivative All-Trans Retinoic Acid Repairs Amyloid-beta-Induced Double-Strand Breaks in Neural Cells and in the Murine Neocortex. *Neural Plast.* **2016**, *2016*, No. 3707406.
(42) Colas, J.; Chessel, N.; Ouared, A.; Gruz-Gibelli, E.; Marin, P.; Herrmann, F. R.; Savioz, A. Neuroprotection against Amyloid-beta-Induced DNA Double-Strand Breaks Is Mediated by Multiple Retinoic Acid-Dependent Pathways. *Neural Plast.* **2020**, *2020*, No. 9369815.

(43) Murphy, M. P.; LeVine, H., 3rd Alzheimer's disease and the amyloid-beta peptide. *J. Alzheimers Dis.* **2010**, *19*, 311−323.
(44) García-Viñuales, S.; Sciacca, M. F. M.; Lanza, V.; Santoro, A. M.; Grasso, G.; Tundo, G. R.; Sbardella, D.; Coletta, M.; Grasso, G.; La Rosa, C.; Milardi, D. The interplay between lipid and Abeta amyloid homeostasis in Alzheimer's Disease: risk factors and therapeutic opportunities. *Chem. Phys. Lipids* **2021**, *236*, No. 105072.
(45) Chew, H.; Solomon, V. A.; Fonteh, A. N. Involvement of Lipids in Alzheimer's Disease Pathology and Potential Therapies. *Front. Physiol.* **2020**, *11*, No. 598.
(46) Nutma, E.; Ceyzeriat, K.; Amor, S.; Tsartsalis, S.; Millet, P.; Owen, D. R.; Papadopoulos, V.; Tournier, B. B. Cellular sources of TSPO expression in healthy and diseased brain. *Eur. J. Nucl. Med. Mol. Imaging* **2021**, 1−18.
(47) Fu, Y.; Wang, D.; Wang, H.; Cai, M.; Li, C.; Zhang, X.; Chen, H.; Hu, Y.; Zhang, X.; Ying, M.; He, W.; Zhang, J. TSPO deficiency induces mitochondrial dysfunction, leading to hypoxia, angiogenesis, and a growth-promoting metabolic shift toward glycolysis in glioblastoma. *Neuro-Oncology* **2020**, *22*, 240−252.
(48) Bode, J.; Veenman, L.; Caballero, B.; Lakomek, M.; Kugler, W.; Gavish, M. The 18 kDa translocator protein influences angiogenesis, as well as aggressiveness, adhesion, migration, and proliferation of glioblastoma cells. *Pharmacogenet. Genomics* **2012**, *22*, 538−550.
(49) Liu, G. J.; Middleton, R. J.; Kam, W. W.; Chin, D. Y.; Hatty, C. R.; Chan, R. H.; Banati, R. B. Functional gains in energy and cell metabolism after TSPO gene insertion. *Cell Cycle* **2017**, *16*, 436−447.
(50) Delavoie, F.; Li, H.; Hardwick, M.; Robert, J. C.; Giatzakis, C.; Peranzi, G.; Yao, Z. X.; Maccario, J.; Lacapere, J. J.; Papadopoulos, V. In vivo and in vitro peripheral-type benzodiazepine receptor polymerization: functional significance in drug ligand and cholesterol binding. *Biochemistry* **2003**, *42*, 4506−4519.
(51) Ammer, L. M.; Vollmann-Zwerenz, A.; Ruf, V.; Wetzel, C. H.; Riemenschneider, M. J.; Albert, N. L.; Beckhove, P.; Hau, P. The Role of Translocator Protein TSPO in Hallmarks of Glioblastoma. *Cancers* **2020**, *12*, No. 2973.

https://doi.org/10.1021/acsomega.1c01678
ACS Omega 2021, 6, 18719−18727